Publications of the Astronomical Society of Japan, 2025, **00**(0), 1–7
https://doi.org/10.1093/pasj/psaf140
Advance access publication date: 2025 December 30

Peculiar SN Ic 2022esa: An explosion of a massive Wolf–Rayet star in a binary as a precursor to a BH–BH binary?†

Keiichi Maeda,[1,*] **Hanindyo Kuncarayakti,**[2,3] **Takashi Nagao,**[2,4,5] **Miho Kawabata,**[6] **Kenta Taguchi,**[1,6] **Kohki Uno,**[1] **and Kishalay De**[7,8]

[1]Department of Astronomy, Kyoto University, Kitashirakawa-Oiwake-cho, Sakyo-ku, Kyoto, Kyoto 606-8502, Japan
[2]Tuorla Observatory, Department of Physics and Astronomy, University of Turku, FI-20014 Turku, Finland
[3]Finnish Centre for Astronomy with ESO (FINCA), University of Turku, FI-20014 Turku, Finland
[4]Aalto University Metsähovi Radio Observatory, Metsähovintie 114, FI-02540 Kylmälä, Finland
[5]Aalto University Department of Electronics and Nanoengineering, P.O. BOX 15500, FI-00076 Aalto, Finland
[6]Okayama Observatory, Kyoto University, 3037-5 Honjo, Kamogatacho, Asakuchi, Okayama 719-0232, Japan
[7]Department of Astronomy, Columbia University, Mail Code 5246, 538 West 120th Street, New York, NY 10027, USA
[8]The Center for Computational Astrophysics, Flatiron Institute, 162 5th Ave., New York, NY 10010, USA

*E-mail: keiichi.maeda@kusastro.kyoto-u.ac.jp

†This research is based in part on data collected at the Subaru telescope, which is operated by the National Astronomical Observatory of Japan. We are honored and grateful for the opportunity of observing the Universe from Maunakea, which has cultural, historical, and natural significance in Hawaii.

Abstract

A class of supernovae (SNe) called SN Ic-CSM are characterized by late-time emergence of narrow emission lines of elements formed in the oxygen core of a massive star. A popular scenario is the interaction of the SN ejecta and O-rich circumstellar medium (CSM), i.e., circumstellar interaction (CSI). Uncovering the progenitor system of SNe Ic-CSM plays a critical role in understanding the final evolution of a massive star to a bare C+O star. In this letter, we present observations of SN 2022esa, which we show is an SN Ic-CSM. Surprisingly, a stable periodicity of ∼32 d is found in its light-curve evolution with a hint of a slowly increasing period over ∼200 d. We argue that the main power source is likely the interaction of the SN ejecta and O-rich CSM, while the energy input by the post-SN eccentric binary interaction within the SN ejecta is another possibility. In either case, we propose a massive Wolf–Rayet (WR) star as the progenitor, in a WR–WR or WR–BH (black hole) binary that will eventually evolve to a BH–BH binary. Specifically, in the CSI scenario, the progenitor system is an eccentric binary system with an orbital period of about a year, leading to the observed periodicity through the modulation in the CSM density structure. We also show that some other objects, superluminous SN I 2018ibb (a pair-instability SN candidate) and peculiar SN Ic 2022jli (the first example showing stable periodic modulation), show observational similarities to SNe Ic-CSM and may be categorized as SN Ic-CSM variants. Complemented with a large diversity in their light-curve evolution, we propose that SNe Ic-CSM (potentially linked to SNe Ibn/Icn) are a mixture of multiple channels that cover a range of properties in the progenitor star, the binary companion, and the binary orbit.

Keywords: binaries: general — stars: evolution — supernovae: general — supernovae: individual (SNe 2022esa, 2018ibb, 2022jli)

1 Introduction

Recent developments in transient observations have revealed the rich diversity of the transient zoo (e.g., Schulze et al. 2025). SN Ic-CSM is a recently found class of objects, characterized by late-time emergence of narrow ($<$ a few 1000 km s^{-1}) emission lines of elements formed in the oxygen core of a massive star (e.g., O and Mg) (Kuncarayakti et al. 2022).[1] Within a still very limited sample, the best studied cases, SNe 2021ocs and 2022xxf, both showed a transition from type Ic (an explosion of a C+O star) to SNe Ic-CSM (Kuncarayakti et al. 2023), establishing their association with C+O star progenitors. In addition to the spectral evolution, they are distinct in the light-curve (LC) evolution from SNe Ic. The interaction between the SN ejecta and CSM (circumstellar interaction: CSI), both rich in oxygen, has been proposed as a power source.

The progenitor channel toward SNe Ic-CSM has not been clarified; it is not even clear whether SNe Ic-CSM form a single population. Also, a relation between SNe Ic-CSM and Ibn/Icn (intense interaction with H-deficient CSM only on a timescale of weeks; Pastorello et al. 2007; Gal-Yam et al. 2022) has not been clarified.

SN 2022esa was discovered on 2022 March 12 (MJD 59650.61)[2] by the Asteroid Terrestrial-impact Last Alert System (ATLAS) (Tonry et al. 2022) in 2MFGC 13525 at $z = 0.02314$. It was classified as an SN Ia-CSM (H-rich CSI-powered SN Ia; Dilday et al. 2012) by Lu et al. (2022). In this letter, we present follow-up observations of SN 2022esa. Its spectral evolution reveals that SN 2022esa is indeed a new member of the SN Ic-CSM class.[3] Its LC also shows

[1] SN Ib 2014C (Margutti et al. 2017) and SN Ic 2017dio (Kuncarayakti et al. 2018b) showed transition to type IIn with strong Balmer emissions in the late phase. In this paper, they are not classified as SNe Ib-CSM or Ic-CSM, which we define as being characterized by narrow emission lines in the H-poor environment.

[2] Dates are shown in UT unless otherwise mentioned.

[3] Recently, Griffith et al. (2025) also mentioned that it is a peculiar SN Ic.

Received: 2025 August 13; **Accepted:** 2025 November 20

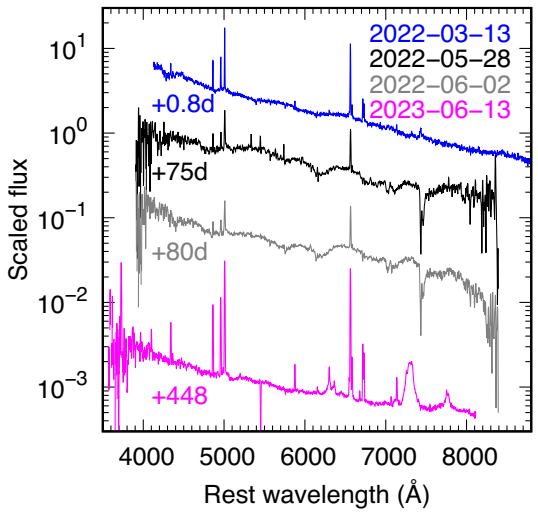

Fig. 1. Spectral evolution of SN 2022esa, including the one (0.8 d) reported by Lu et al. (2022). For the FOCAS spectrum for day 448, the original (SN+HII) spectrum is shown.

unique features, including periodic modulation. We present these characteristic observational features, and discuss its main power source and the progenitor system.

2 Observations and data reduction

Spectra of SN 2022esa were obtained on 2022 May 28 ($t = 75$ d)[4] and June 2 ($t = 80$ d), using the Kyoto Okayama Optical Low-dispersion Spectrograph with optical-fiber Integral Field Unit (KOOLS-IFU; Matsubayashi et al. 2019) mounted on the Kyoto University 3.8 m Seimei telescope (Kurita et al. 2020). We used the VPH-blue grism with a wavelength coverage of ∼4000–8500 Å and a spectral resolution of ∼600. The total exposure time was 2700 s in each night. A late-time spectrum was obtained on 2023 June 13 ($t = 448$ d), using the Faint Object Camera And Spectrograph (FOCAS) mounted on the Subaru telescope. We used a 0.″8 slit and the B300 grism with no order-cut filter, covering 3650–8300Å with a spectral resolution of ∼500. The total exposure time was 3600 s. Additionally, we obtained V- (120 s) and R-band (180 s) images on the same night with FOCAS.

The reduction of the FOCAS data was performed in the standard manner with IRAF[5] (see Maeda & Kawabata 2022). The reduction of the KOOLS-IFU data follows similar procedures, with the Hydra package (Barden 1994) and custom routines.[6]

The spectra of SN 2022esa (figure 1) show a number of narrow emission lines from an underlying unresolved H II region. For the FOCAS spectrum, the contamination is especially substantial given the decreasing SN flux, and thus we subtracted it with a spectrum of a nearby H II region taken in the same 2D image. The flux was converted to the absolute scale by assuming a distance modulus of 35.24 mag and the Milky Way (MW) extinction with $E(B-V) = 0.6$ mag. We assume that the extinction within the host is negligible; in addition to the absence of strong Na ID absorption, the Balmer decrement measured from the underlying H II region is consistent with the MW-only extinction.

The light curves (LCs) of SN 2022esa (figure 2) were constructed as follows. For the early phase up to $t \sim 200$ d, we used public resources. The ATLAS o- and c-band magnitudes were obtained using the ATLAS forced photometry server[7] (Tonry et al. 2018; Shingles et al. 2021). The Zwicky Transient Facility (ZTF) g- and r-band magnitudes were obtained through the ALeRCE explorer[8] (Förster et al. 2021). We used the FOCAS spectrum to estimate the "SN-only" magnitude in the late phase ($t = 448$ d). First, spectrophotometry on the "SN + H II region" resulted in $V \sim 20.8$ and $R \sim 20.3$ mag (in Vega), being consistent with the photometry performed on the V and R images ($V = 21.10 \pm 0.12$ and $R = 20.29 \pm 0.14$ mag). We then performed spectrophotometry on the H II-region-subtracted spectrum, obtaining pure-SN magnitudes of $g = 23.6 \pm 0.3$ and $r = 23.3 \pm 0.3$ mag (in AB).

We also constructed infrared LCs using the data from the NEOWISE mission (Mainzer et al. 2014) in the W1 (3.4 μm) and W2 (4.6 μm) bands, taken by the Wide-field Infrared Survey Explorer (WISE; Wright et al. 2010). We performed point-spread function (PSF) photometry at the position of the source in the NEOWISE difference images (De et al. 2020, 2023).

3 Results

3.1 Modulation in the light curve

Figure 2 shows bumpy structures in the LC evolution, a characteristic that is rarely seen in SNe. The evolution is coherent in different bands; excluding the ATLAS c-band data that are not well sampled, we performed a periodgram analysis. We first fitted the overall LC of a given band by a polynomial function of fifth order, creating the mean LC. This mean LC was subtracted from the original LC, and then the residual was further divided by the mean LC. The resulting "fractional-residual" LCs for the ATLAS o-band and ZTF r- and g-bands are shown in figure 3 (left). Surprisingly, SN 2022esa showed clear periodicity over multiple cycles, which has been reported previously only for the peculiar SN Ic 2022jli (Moore et al. 2023; Chen et al. 2024).[9]

We performed Lomb–Scargle (LS) periodogram analyses for the residual LCs separately in the o-, r-, and g-band data, using the LombScargle module implemented in astropy. This was done iteratively by rejecting outliers by 3σ clipping in the data-model residual. A sharp peak in the power spectrum is found at the period that is consistent among all the three bands; 31.8 ± 2.8 d (o), 32.0 ± 2.1 d (r), and 31.0 ± 2.2 d (g) (figure 3, middle). To further investigate possible quasi-periodic behavior, we performed a sliding-window analysis with a window size of 100 d and a step size of 25 d on the ZTF-r data. As shown in figure 3 (right), the data are consistent with no change in the period within 1σ, while there is a hint of a possible increase in the period over time.[10]

[4] In this letter, we define the phase (t) of SN 2022esa as measured from the discovery date. The timescale (e.g., LCs shown in figures) is shown in the SN rest frame, corrected for redshift, for all the objects.

[5] IRAF is distributed by the National Optical Astronomy Observatory, which is operated by the Association of Universities for Research in Astronomy (AURA) under a cooperative agreement with the National Science Foundation.

[6] ⟨http://www.o.kwasan.kyoto-u.ac.jp/inst/p-kools/reduction-201806/index.html⟩.

[7] ⟨https://fallingstar-data.com/forcedphot/⟩.

[8] ⟨https://alerce.science/⟩.

[9] Another example, the type I superluminous SN (SLSN-I) 2024afav, has recently been reported to show a quasi-periodic LC (Farah et al. 2025). See also West et al. (2023) for SLSN-I 2020qlb.

[10] The sliding-window analysis of the ATLAS-o data resulted in the same conclusion, with a larger error in the derived period.

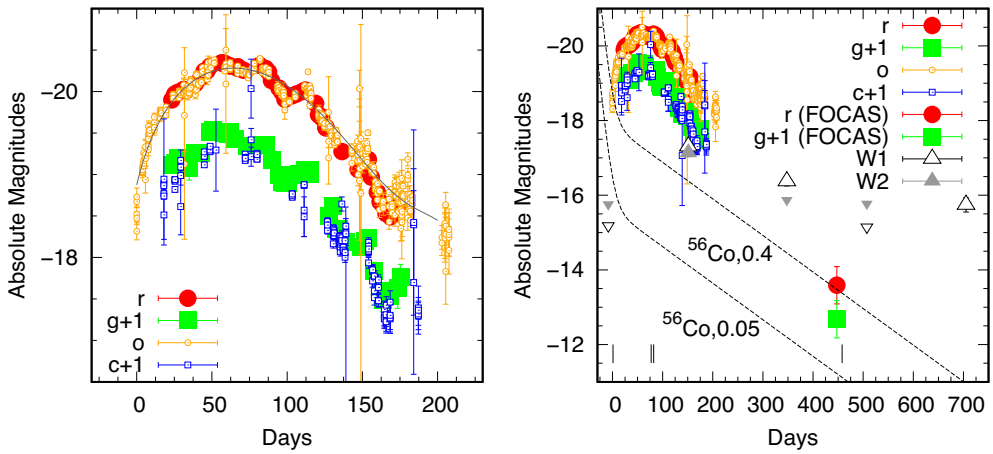

Fig. 2. Multi-band LCs of SN 2022esa around the peak (left) and those including the late-time measurements (right). The *g*- and *c*-band magnitudes are shifted by +1 mag for presentation. In the left panel, the mean LC (for ATLAS-*o*) is shown by a gray line. In the right panel, the WISE W1 (3.4 μm) and W2 (4.6 μm) magnitudes (triangles) and 3 σ upper limits (inversed triangles) are shown. Also shown are the full-deposition ^{56}Ni/Co/Fe decay curves for $M(^{56}\mathrm{Ni}) = 0.4$ and 0.05 $M_\odot$, assuming that the explosion date is 15 d before the discovery. The epochs when the spectra were taken are indicated by short vertical lines on the *x*-axis.

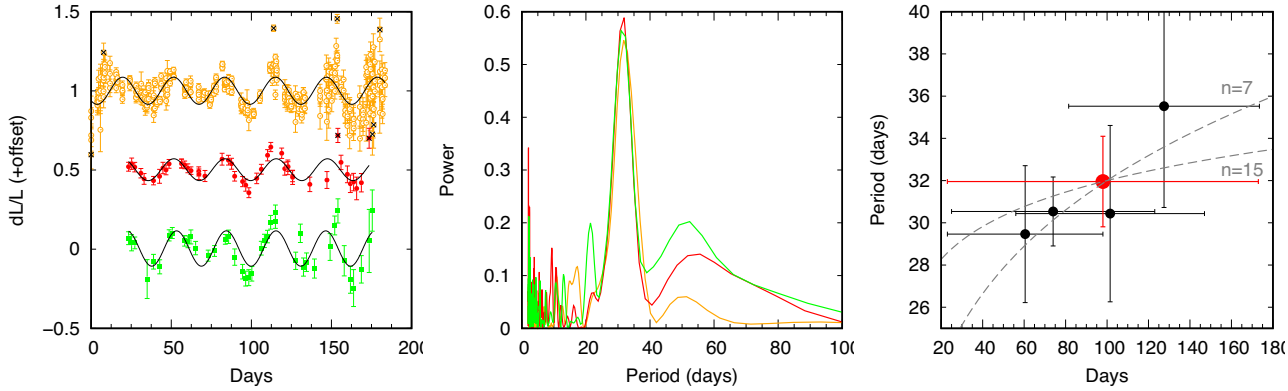

Fig. 3. Fractional-residual LCs in the ATLAS-*o* (orange), ZTF-*r* (red), ZTF-*g* (green), and the best-fitting sine curves through the LS analyses are shown in the left panel. The data points that were rejected through the LS analyses are shown by crosses. In the middle panel, the power spectra, using the same color coordinates as those used in the left panel, are shown. In the right panel, the periods obtained through the sliding-window analysis (black) as well as using the full time window (red) are shown for the ZTF-*r* data. The CSI-model predictions for the period change are shown by the dashed lines (see the main text).

In the case of SN 2022jli, the origin of the modulation has not been conclusively clarified (Moore et al. 2023; Cartier et al. 2024), but a "post-SN" binary interaction between the compact object left behind after the explosion and the bound companion star has been proposed (Chen et al. 2024). As compared to SN 2022jli, the modulation seen here has several distinct properties. SN 2022jli showed (1) a shorter period (12.4 d), and (2) an asymmetric temporal profile with a fast rise ($\leq$3 d), while it is consistent with a symmetric profile for SN 2022esa. Further, (3) the modulation was observed in the late phase after $\sim$50 d in SN 2022jli, while the early rising LC of SN 2022esa is consistent with having undergone modulation already. There are also other differences between SNe 2022esa and 2022jli in the overall LC and spectral evolutions, which will be discussed in subsequent sections.

Temporal variations are sometimes seen in radio LCs of stripped-envelope SNe (SESNe, i.e., SNe IIb/Ib/Ic) (Wellons et al. 2012), and the quasi-periodic modulation has been reported for a few SNe (Ryder et al. 2004; Kotak & Vink 2006; Soderberg et al. 2006). The behavior has been generally interpreted to be caused by the modulation in the CSM density structure. Especially popular is the scenario that involves a luminous blue variable-like progenitor (Kotak & Vink 2006). Indeed, the temporal variation in the LC, while usually without periodic behavior, is common among SNe Ic-CSM (see subsection 3.3); the H-poor CSI in a non-smooth CSM distribution is a popular scenario (Kuncarayakti et al. 2023).

3.2 SN 2022esa as a new member of SNe Ic-CSM

SN 2022esa already showed broad spectral features in the early phase with no clear sign of Hα from the SN (figure 1). The broad features were further developed at the maximum phase. Finally, in the late epoch, strong and narrow (but resolved) lines (FWHM $\sim$ 2000 km s^{-1}) from intermediate-mass elements (IMEs) such as O and Ca were clearly detected; these properties are inconsistent with SN Ia-CSM, but rather indicate that SN 2022esa was associated with O-rich environments, i.e., SN Ic or its variants.

We compare the spectral evolution of SN 2022esa with those of SNe Ic-CSM and a few related objects (figure 4). SN Icn 2021ckj is a rapidly decaying SN where the interac-

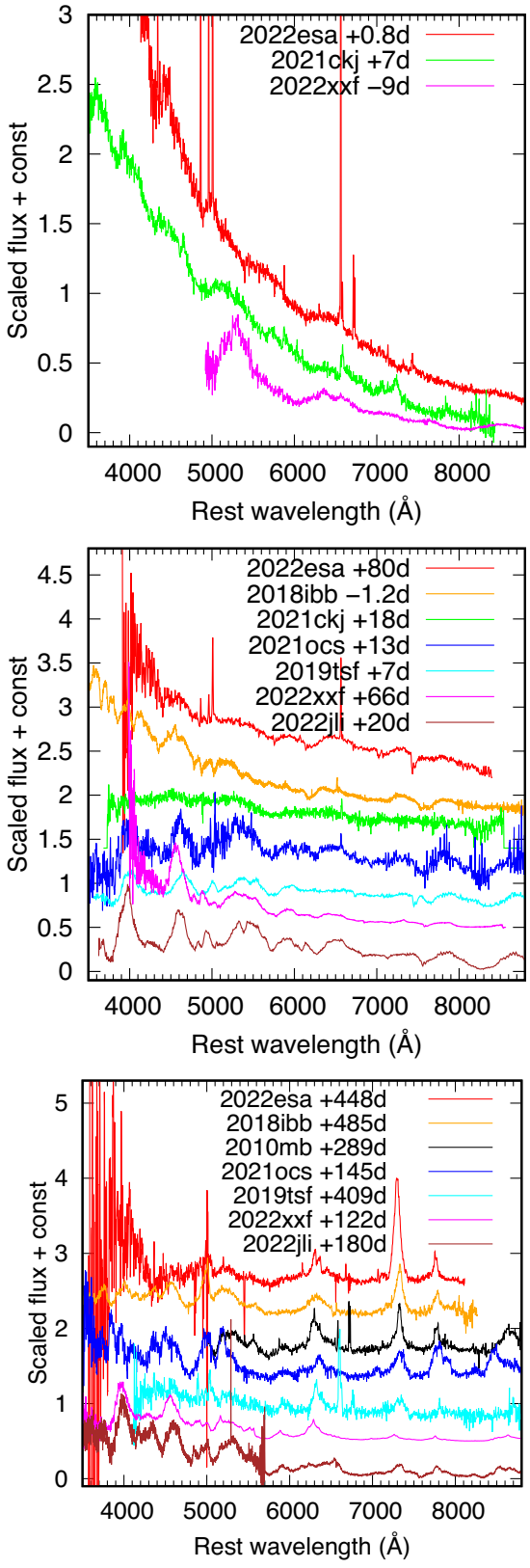

Fig. 4. Comparison of the spectra of SN 2022esa to SNe Ic-CSM and related objects in the early (top), peak/intermediate (middle), and late phases (bottom). In the bottom panel, the H II region-subtracted spectrum is shown. The data of the comparison objects are from the literature in subsection 3.2, and downloaded through WISeREP (Yaron & Gal-Yam 2012) or provided by the authors of the literature. The phases for the comparison objects are measured from the peak light (in their rest frames).

tion with "confined" C-rich CSM is the main energy source (Pellegrino et al. 2022; Nagao et al. 2023). SNe 2010mb (Ben-Ami et al. 2014), 2021ocs (Kuncarayakti et al. 2022), and 2022xxf (Kuncarayakti et al. 2023) were classified as SNe Ic-CSM based on their late-time spectra. They showed flat or slowly decaying LCs even with multiple peaks. From these features, SNe Ic-CSM have been proposed to be SNe Ic exploded within dense and extended O-rich CSM. SNe 2021ocs and 2022xxf did not show the signatures of strong CSI in the early phase, and were classified as a canonical SN Ic and a broad-lined SN Ic (SN Ic-BL) initially, pointing to the diverse nature of the SN ejecta in the SN Ic-CSM class. SN 2019tsf is a peculiar SN Ib in its LC evolution (Sollerman et al. 2020), later showing the spectral features of SNe Ic-CSM (Pyykkinen et al. 2025). SLSN-I 2018ibb has been suggested to be a pair-instability SN (PISN) (Schulze et al. 2024; Nagele et al. 2024), with the late-time spectrum indicating an additional power provided by the H-poor CSI (Chugai 2024). Finally, SN Ib 2022jli, the first SN showing clear periodicity, is also shown for comparison (Moore et al. 2023; Chen et al. 2024).

SN 2022esa shows a striking similarity to SNe Ic-CSM. The earliest spectrum is overall similar to the spectrum of SN 2022xxf at the first peak. The broad features also show a resemblance to SN Icn 2021ckj, while the narrow emission lines from highly ionized carbon are missing in SN 2022esa. These similarities indicate that SN 2022esa is related to an oxygen-star progenitor, i.e., SN Ic.

The spectrum around the peak of SN 2022esa shows clear similarity to those of SNe Ic-CSM 2021ocs and 2022xxf. Interestingly, the candidate PISN 2018ibb and the "periodic" SN Ic 2022jli are similar to SN Ic-CSM objects and SN 2022esa, implying a link between these peculiar objects and the SN Ic-CSM class; we suggest that they could indeed be variants of SNe Ic-CSM, potentially sharing a similar power source and/or spectral-formation process.

Finally, the late-time spectrum (+448 d) shows a striking similarity to those of SNe Ic-CSM and (somehow surprisingly) SN 2018ibb, characterized by narrow emission lines from O and IMEs, together with the blue Fe complex. SN Ib 2019tsf has started showing SN Ic-CSM characteristics, and it might be classified as an SN Ib-CSM. Interestingly, SN 2022jli also shows an overall similar spectrum to SNe Ic-CSM; however, it shows important differences, i.e., broad Hα emission instead of [O I].

3.3 Possible power sources

The large luminosity (<-20 mag) and long duration (<-19 mag for $\sim$150 d) indicate the radiated energy of SN 2022esa reaching at least $\sim 3 \times 10^{50}$ erg. In addition, the color remained rather constant and blue ($g-r$ and $c-o \sim 0$ mag) throughout the period up to $t \sim 500$ d. The CSI is a promising candidate to explain these properties. Figure 5 compares the LCs of SN 2022esa and related objects, including the "H-rich CSI" SN IIn 2010jl (Zhang et al. 2012) and Ia-CSM 2020uem (Uno et al. 2023). In addition to the lack of the H features in the spectra, the LC evolution also indicates that SN 2020esa is of neither the SN Ia-CSM nor the SN IIn class.[11]

Some SNe Ic-CSM show two or more peaks, which has been associated with two different energy sources—^{56}Ni/Co/Fe heating at the first peak, and the O-rich CSI thereafter. The most likely energy source for SN 2022esa is thus the O-rich

[11] We note, however, that the LCs of SNe IIn are very diverse.

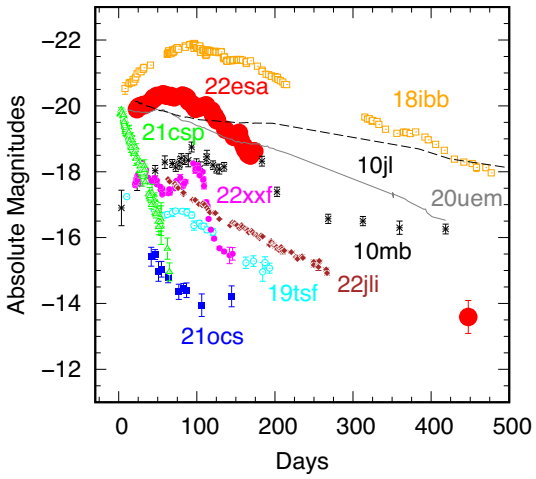

Fig. 5. Comparison of the *r*-band LC of SN 2022esa with SNe Icn and Ic-CSM (and related objects). The color coordinates are the same as those in figure 4 (note that SN Icn 2021ckj is replaced by SN Icn 2021csp; Perley et al. 2022). Also shown here are SNe Ia-CSM 2020uem and IIn 2010jl.

CSI, and the LC periodicity reflects the fluctuation in the CSM density. Under this scenario, we have two additional constraints: (1) the large peak luminosity indicates a very high mass-loss rate, reaching $\geq$0.01–0.1 $M_\odot$ yr^{-1} (Maeda et al. 2013; Uno et al. 2023) just before the explosion (unlike SNe 2021ocs and 2022xxf showing the late-time emergence of the CSI), and (2) it requires a stable periodic phenomenon to introduce the CSM density fluctuation (unlike SN 2022xxf showing a bumpy LC but without clear periodicity).

We note two additional hints supporting the CSI scenario: (1) The properties of the radio emission (Griffith et al. 2025), $\sim 10^{28}$ erg s^{-1} Hz^{-1} at $\sim$1.5 yr at 6 GHz, are typical of SNe IIn (Chevalier et al. 2006; Maeda 2013). (2) IR excess is seen in the late phase (figure 2), similar to that frequently observed in SNe IIn. The IR emission signals dusty environments associated with dense CSM either through an echo from pre-existing CS dust (at a larger distance; Maeda et al. 2015) or through the reprocessing of the optical photons to the IR by newly formed dust (at a smaller scale; Maeda et al. 2013). Given the blue optical color even in the late phase, pre-existing dust is a more likely scenario. We will further investigate the nature of the IR excess in a separate paper.

If the pre-SN mass loss was perfectly periodic with no change in the mass-loss velocity (V_w), the CSM "shells" would be equally spaced. Then, the observed LC modulation period would be inversely proportional to the SN shock velocity V_{SN}. Therefore, we expect the period to be constant (for constant V_{SN}) or increasing (for decreasing V_{SN}). For example, for the decelerated SN shock in a steady-state wind-like CSM, $V_{SN} \propto t^{-1/(n-2)}$ where n is the density slope in the SN ejecta ($\rho_{SN} \propto v^{-n}$). Figure 3 (right) shows the predictions for $n = 7$ and 15 covering a range of SN-ejecta properties (Chevalier 1982). The observed period is consistent with this picture (i.e., no change within the error, but with a hint of an increasing period).

The "post"-SN binary interaction scenario proposed for SN 2022jli, where the "central engine" through the post-SN binary interaction powers the LC periodically, is not rejected. However, the main argument against the CSI scenario for SN 2022jli, namely a variability shorter than the light-traveltime, does not apply for SN 2022esa. Also, given its high luminosity, SN 2022esa would require a very strong binary interaction and a high mass-transfer rate, and the period may likely decrease rapidly, inconsistent with the constant or slowly increasing period in SN 2022esa.

3.4 SN-site environment

We measured metallicity at the SN site and the nearby H II region, using the O3N2 and N2 calibrations from Marino et al. (2013). We found that the metallicities for the two regions are the same within error. Two calibrations provide consistent results: $12 + \log(\mathrm{O/H}) \sim 8.3 \pm 0.2$ dex (N2) and $12 + \log(\mathrm{O/H}) \sim 8.2 \pm 0.2$ dex (O3N2), i.e., $Z \sim 0.4$–$0.5\ Z_\odot$. This is similar to the cases of some strongly interacting SNe, e.g., Type IIn SN 2010jl (Stoll et al. 2011; Maeda et al. 2013).

The equivalent width of the Hα emission line (HαEW) is frequently used to infer the age of the stellar population and the lifetime of the progenitor star (see, e.g., Kuncarayakti et al. 2018a). The measured HαEW of the SN 2022esa environment is around 600 Å. Using the Starburst99 single-burst model (Leitherer et al. 1999) at half solar metallicity, this corresponds to a stellar population age of around 4.7 Myr, and thus to the lifetime of a $\sim$50 $M_\odot$ star. Such a massive star is expected to evolve to a massive WR star (Heger et al. 2003). While the single-burst model can overestimate the progenitor mass, the young stellar population age suggests a massive star origin for SN 2022esa.

4 Discussion

4.1 Progenitor system: WR–WR or WR–BH binary?

Under the CSI scenario, the LC covering $\sim$1 yr reflects the activity of the progenitor (system) in the final $\sim(V_{SN}/V_w)$ yr $\sim$10 yr, where $V_{SN} \sim 10000$ km s^{-1} and $V_w \sim 1000$ km s^{-1} are assumed. The LC modulation period is translated into $\sim$1 yr for the variability period of the pre-SN mass loss. A binary interaction, where one component is the C+O-star SN progenitor, is an appealing possibility to create such a stable periodicity.

The circularized close binary, which is believed to be a major channel toward SESNe (Fang et al. 2019), would not create a stable periodicity. Alternatively, a highly eccentric binary experiences repeated binary interactions every time the system passes the pericenter, potentially resulting in a periodic mass loss. This suggests that the progenitor of SN 2022esa likely evolved to a C+O star without strong binary interaction (which circularizes the orbit)—a massive WR star that has lost the outer H and He envelopes by its strong wind. Assuming the total mass of the pre-SN binary systems as $\sim$20–30 $M_\odot$, the average pre-SN binary separation must have been $\sim 500\ R_\odot$. This again points to a massive WR star progenitor that can avoid becoming a red supergiant, thus not experiencing a Roche-lobe overflow and/or common envelope (CE) that will circularize the orbit and lead to a compact binary.

No trace of hydrogen may suggest an H-deficient companion star, i.e., either a WR–WR system (analogous to the eccentric WR–WR binary Apep; Callingham et al. 2020) or a WR–BH system, noting that a neutron-star (NS) companion is unlikely if the progenitor is a massive WR. While the (still rare) observed WR–BH systems generally show close circularized orbits (Prestwich et al. 2007; Binder et al. 2021), this may

simply be due to observational biases; for O-star–WR binaries (as a progenitor to WR–BH binaries) such as WR140, a period of a year to decades with an eccentric orbit is common (e.g., Williams et al. 2009). The ejecta mass of SN 2022esa would not exceed half of the total mass for the binary system considered here, and the binary likely survived after SN 2022esa. Therefore, the proposed WR–WR or WR–BH system will ultimately lead to the formation of a BH–BH binary.

The LC decay of SN 2022esa is much faster than SNe interacting with extended CSM like SNe 2010jl and 2020uem. This indicates a steep CSM density gradient and an increasing mass-loss rate toward the SN. The binary interaction was thus "switched on" in the last decade before the SN. Such a synchronization requires that the final evolution of the progenitor drove the binary interaction. One possibility is inflation of the progenitor star or some sort of activity in the final phase (Ouchi & Maeda 2019) that could lead to an increasingly strong binary interaction toward the SN. For example, a massive WR progenitor has been proposed for SNe Ibn/Icn (Pastorello et al. 2007; Gal-Yam et al. 2022)—putting such a star in an eccentric binary would lead to further enhancement of the mass loss and could lead to objects like SN 2022esa.

In the "post-SN" binary interaction scenario, the observed period reflects the post-SN binary period—the average separation of $\sim 100\,R_\odot$. Given the lack of Hα, the companion star would also be a C+O star; it is unlikely that both stars evolve to C+O stars through strong binary interaction, and a massive WR–WR binary is a favored system in this scenario too. A few caveats should be noted: the emergence of Hα might be a transient feature and could simply be missed, or the Hα may be hidden as the binary interaction happens deep inside the ejecta. In these cases, a WR–O/B-star binary progenitor system would also be possible. Either way, again the system may ultimately evolve to a BH–BH binary.

4.2 SN Ic-CSM diversities: Multiple populations?

The speed of the spectral evolution is diverse among SNe Ic-CSM. Also, the early-phase spectra show some diversities, e.g., SNe 2021ocs and 2022xxf, classified as normal Ic and Ic-BL. While overall features are shared in the late phase, there are also differences; in figure 4, only SN 2022jli shows Hα and a lack of [O I]6300/6363.[12] It is also seen that SN 2018ibb shows broader features than the others.

SNe Ic-CSM show a huge diversity in the LC evolution (figure 5); the peak magnitude, the timescale, and the evolution morphology are diverse. This may indicate that SNe Ic-CSM are likely to be a mixture of different populations originating in multiple progenitor channels. For most of them, the O-rich CSI is likely the main power source, with diverse properties in the CSM (and thus in the mass-loss history). Even the underlying power source may not be unique, possibly including the post-SN binary interaction. These channels may include a massive WR–WR or WR–BH binary (proposed here for SN 2022esa), a standard (relatively low-mass) SESN binary channel but extreme conditions for the binary mass transfer (perhaps involving a CE), a WR + normal (perhaps O) star binary (proposed for SN 2022jli), and a PISN (proposed for 2018ibb). In most cases, the binarity seems to be a key; depending on the nature of the binary components (types of stars and masses) and the orbit (separation and eccentricity), a huge diversity within the "SN Ic-CSM" class (and possibly including Ibn/Icn) may be created.

[12] It is thus not SN Ic-CSM. We note, however, the emergence of [O I] in the later epoch (Cartier et al. 2024) as another indication of its link to SNe Ic-CSM.

5 Concluding remarks

In this letter, we have presented unique features of SN 2022esa. In addition to the bright optical emission, it showed a stable periodicity ($\sim$32 d) in the LC, with a possible hint of a slowly increasing period over $\sim$200 d. Further, the spectra evolved into the characteristic "SN Ic-CSM" late-time spectrum, showing blue Fe bumps and narrow emission lines from IMEs.

For the power source, both the CSI and the post-SN binary interactions remain possible, while the CSI is more likely. In either case, we suggest a massive WR progenitor star, in a binary with either another WR or a BH. For the CSI scenario, we further require a highly eccentric orbit. Therefore, SN 2022esa may represent a progenitor system that will eventually evolve to a BH–BH binary.

We showed that the SNe Ic-CSM class has a huge diversity, pointing out that SNe 2018ibb (a PISN candidate) and 2022jli (another example showing a clear periodicity) have similarities to SNe Ic-CSM. We suggest that SNe Ic-CSM represent a mixture of multiple populations. The progenitor mass may span a range from the "canonical SESN progenitor" ($M_{\rm ZAMS} < 20\,M_\odot$) to a massive WR star ($>20\,M_\odot$), or even to the PISN regime ($>100\,M_\odot$). Furthermore, for many of them, binary interaction seems to play a key role, adding a source of the diversity depending on the binary configuration that may further connect them to SNe Ibn/Icn.

SNe Ic-CSM can thus represent a rich and diverse zoo of massive binary evolution, including progenitors toward BH–BH binaries. As such, further studying them, both observationally and theoretically, will provide a major contribution to uncover the still-unclarified final evolution of massive stars, roles of binarity, and formation channels of double compact-object binaries.

Funding

KM acknowledges support from JSPS KAKENHI grants (JP24KK0070, JP24H01810, JP24K00682, and JP20H00174). HK was funded by the Research Council of Finland projects 324504, 328898, and 353019. The work is partly supported by the JSPS Open Partnership Bilateral Joint Research Projects between Japan and Finland (KM and HK; JPJSBP120229923).

Data availability

The data underlying this article will be available through WiseRep.

Acknowledgments

The authors thank Kentaro Aoki for his excellent assistance with the observation with the Subaru telescope (under the program S23A-023), and Niko Pyykkinen for providing the unpublished spectrum of SN 2019tsf. The data from the Seimei telescope were obtained under the KASTOR (Kanata And Seimei Transient Observation Regime) project (under the programs 22A-N-CT09 and 22A-K-0030). The Seimei telescope

is jointly operated by Kyoto University and the Astronomical Observatory of Japan (NAOJ), with assistance provided by the Optical and Near-Infrared Astronomy Inter-University Cooperation Program. Some public data are obtained from WISeREP (https://www.wiserep.org).

References

Barden, S. C. 1994, ASP Conf. Ser., 55, 130
Ben-Ami, S., et al. 2014, ApJ, 785, 37
Binder, B. A., et al. 2021, ApJ, 910, 74
Callingham, J. R., Crowther, P. A., Williams, P. M., Tuthill, P. G., Han, Y., Pope, B. J. S., & Marcote, B. 2020, MNRAS, 495, 3323
Cartier, R., et al. 2024, arXiv:2410.21381
Chen, P., et al. 2024, Nature, 625, 253
Chevalier, R. A. 1982, ApJ, 258, 790
Chevalier, R. A., Fransson, C., & Nymark, T. K. 2006, ApJ, 641, 1029
Chugai, N. N. 2024, Astron. Lett., 50, 502
De, K., et al. 2020, PASP, 132, 025001
De, K., et al. 2023, Nature, 617, 55
Dilday, B., et al. 2012, Science, 337, 942
Fang, Q., Maeda, K., Kuncarayakti, H., Sun, F., & Gal-Yam, A. 2019, Nature Astron., 3, 434
Farah, J. R., et al. 2025, arXiv:2509.08051
Förster, F., et al. 2021, AJ, 161, 242
Gal-Yam, A., et al. 2022, Nature, 601, 201
Griffith, O., et al. 2025, ApJ, 995, 54
Heger, A., Fryer, C. L., Woosley, S. E., Langer, N., & Hartmann, D. H. 2003, ApJ, 591, 288
Kotak, R., & Vink, J. S. 2006, A&A, 460, L5
Kuncarayakti, H., et al. 2018a, A&A, 613, A35
Kuncarayakti, H., et al. 2018b, ApJ, 854, L14
Kuncarayakti, H., et al. 2022, ApJ, 941, L32
Kuncarayakti, H., et al. 2023, A&A, 678, A209
Kurita, M., et al. 2020, PASJ, 72, 48
Leitherer, C., et al. 1999, ApJS, 123, 3
Lu, J., et al. 2022, Transient Name Server Classification Report, No. 2022-733
Maeda, K. 2013, ApJ, 762, 14
Maeda, K., & Kawabata, M. 2022, ApJ, 941, 15
Maeda, K., et al. 2013, ApJ, 776, 5
Maeda, K., Nozawa, T., Nagao, T., & Motohara, K. 2015, MNRAS, 452, 3281
Mainzer, A., et al. 2014, ApJ, 792, 30
Margutti, R., et al. 2017, ApJ, 835, 140
Marino, R. A., et al. 2013, A&A, 559, A114
Matsubayashi, K., et al. 2019, PASJ, 71, 102
Moore, T., et al. 2023, ApJ, 956, L31
Nagao, T., et al. 2023, A&A, 673, A27
Nagele, C., Umeda, H., & Maeda, K. 2024, ApJ, 972, 11
Ouchi, R., & Maeda, K. 2019, ApJ, 877, 92
Pastorello, A., et al. 2007, Nature, 447, 829
Pellegrino, C., et al. 2022, ApJ, 938, 73
Perley, D. A., et al. 2022, ApJ, 927, 180
Prestwich, A. H., et al. 2007, ApJ, 669, L21
Pyykkinen, N., Nagao, T., Kuncarayakti, H., Stritzinger, M. D., Bose, S., Kangas, T., Reguitti, A., & Salmaso, I. 2025, A&A, submitted
Ryder, S. D., Sadler, E. M., Subrahmanyan, R., Weiler, K. W., Panagia, N., & Stockdale, C. 2004, MNRAS, 349, 1093
Schulze, S., et al. 2024, A&A, 683, A223
Schulze, S., et al. 2025, Nature, 644, 634
Shingles, L., et al. 2021, Transient Name Server AstroNote, No. 7
Soderberg, A. M., Chevalier, R. A., Kulkarni, S. R., & Frail, D. A. 2006, ApJ, 651, 1005
Sollerman, J., et al. 2020, A&A, 643, A79
Stoll, R., Prieto, J. L., Stanek, K. Z., Pogge, R. W., Szczygieł, D. M., Pojmański, G., Antognini, J., & Yan, H. 2011, ApJ, 730, 34
Tonry, J. L., et al. 2018, PASP, 130, 064505
Tonry, J., et al. 2022, Transient Name Server Discovery Report, No. 2022-685
Uno, K., et al. 2023, ApJ, 944, 203
Wellons, S., Soderberg, A. M., & Chevalier, R. A. 2012, ApJ, 752, 17
West, S. L., et al. 2023, A&A, 670, A7
Williams, P. M., et al. 2009, MNRAS, 395, 1749
Wright, E. L., et al. 2010, AJ, 140, 1868
Yaron, O., & Gal-Yam, A. 2012, PASP, 124, 668
Zhang, T., et al. 2012, AJ, 144, 131

Received: 2025 August 13; Accepted: 2025 November 20